JVI Journals.ASM.org

Occurrence and Reassortment of Avian Influenza A (H7N9) Viruses Derived from Coinfected Birds in China

Wei Liu,[a] Hang Fan,[a] Jayna Raghwani,[b] Tommy Tsan-Yuk Lam,[c] Jing Li,[a] Oliver G. Pybus,[b] Hong-Wu Yao,[a] Ying Wo,[a] Kun Liu,[a] Xiao-Ping An,[a] Guang-Qian Pei,[a] Hao Li,[a] Hong-Yu Wang,[a] Jian-Jun Zhao,[a] Tao Jiang,[a] Mai-Juan Ma,[a] Xian Xia,[a] Yan-De Dong,[a] Tong-Yan Zhao,[a] Jia-Fu Jiang,[a] Yin-Hui Yang,[a] Yi Guan,[c] Yigang Tong,[a] Wu-Chun Cao[a]

State Key Laboratory of Pathogen and Biosecurity, Beijing Institute of Microbiology and Epidemiology, Beijing, People's Republic of China[a]; Department of Zoology, University of Oxford, Oxford, United Kingdom[b]; State Key Laboratory of Emerging Infectious Diseases, Centre of Influenza Research, School of Public Health, The University of Hong Kong, Hong Kong SAR, China[c]

ABSTRACT

Over the course of two waves of infection, H7N9 avian influenza A virus has caused 436 human infections and claimed 170 lives in China as of July 2014. To investigate the prevalence and genetic diversity of H7N9, we surveyed avian influenza viruses in poultry in Jiangsu province within the outbreak epicenter. We found frequent occurrence of H7N9/H9N2 coinfection in chickens. Molecular clock phylogenetic analysis confirms coinfection by H7N9/H9N2 viruses and also reveals that the identity of the H7N9 outbreak lineage is confounded by ongoing reassortment between outbreak viruses and diverse H9N2 viruses in domestic birds. Experimental inoculation of a coinfected sample in cell culture yielded two reassortant H7N9 strains with polymerase segments from the original H9N2 strain. Ongoing reassortment between the H7N9 outbreak lineage and diverse H9N2 viruses may generate new strains with the potential to infect humans, highlighting the need for continued viral surveillance in poultry and humans.

IMPORTANCE

We found frequent occurrence of H7N9/H9N2 coinfection in chickens. The H7N9 outbreak lineage is confounded by ongoing reassortment between H7N9 and H9N2 viruses. The importance of H9N2 viruses as the source of novel avian influenza virus infections in humans requires continuous attention.

The avian influenza A (H7N9) virus has caused 436 human infections and claimed 170 lives in China as of 31 July 2014. A second wave of human infection is under way in mainland China, suggesting the potential for further epidemic spread of this strain (1). This novel influenza A virus had not been detected previously in animals or humans and is a reassortant of multiple influenza A virus lineages, including H7, N9, and H9N2 subtype viruses circulating in avian populations (2–7). Although a few studies have now surveyed the genetic diversity of this new strain (8, 9), the exact time, location, and host species distribution of the H7N9 virus remain uncertain, largely due to the relative paucity of systematic surveillance data before the detection of the outbreak. The geographic distribution of cases of human infection is extensive and covers a 1,000-km stretch of coastal China from Shanghai to Beijing, indicating that the virus is already spatially widespread. Domestic ducks have been shown to harbor predecessor strains of the H7N9 influenza A virus that subsequently underwent reassortment and cross-species transmissions to chicken populations. Chickens are thought to be the immediate source of the zoonotic infections reported in humans (7). Because the virus is of low pathogenicity in birds and spreads among avian populations without causing noticeable mortality (10), it is important to identify the bird reservoirs that serve as disease sources in order to reduce human exposure.

Recent studies have demonstrated that current H7N9 viruses most likely originated through multiple reassortment events, with the internal genes reassorted from circulating H9N2 strains in poultry (9, 11). The continuing circulation of H7N9 has resulted in the coexistence of H7N9 and H9N2 viruses in poultry populations and in further reassortment between them. Understanding the complex reassortment history of H7N9 necessitates widespread influenza virus surveillance, not only of H7N9 influenza viruses but also of H9N2 strains. Cocirculation and coinfection of H7N9 and H9N2 viruses, despite their importance for the generation and emergence of novel influenza virus lineages, have been reported only from Zhejiang (11), Shandong (7), and Guangdong (12). The molecular epidemiology of H7N9 and H9N2 viruses in Jiangsu, a key region in the outbreak epicenter in eastern China, is largely unclear.

We conducted a field survey of avian influenza virus infection in poultry from Jiangsu province, which is within the outbreak epicenter in eastern China. Samples were obtained in April 2013 during the first wave of H7N9 infection in humans. Cloacal and tracheal swabs were collected from various species of poultry at a number of bird markets and farms and screened by real-time quantitative PCR (RT-qPCR) for H7N9 avian influenza A viruses. Selected positive samples were subjected to further genome se-

Received 25 June 2014 **Accepted** 2 September 2014

Published ahead of print 10 September 2014

Editor: B. Williams

Address correspondence to Yigang Tong, tong.yigang@gmail.com, or Wu-Chun Cao, caowc@bmi.ac.cn.

W.L., H.F., J.R., and T.T.-Y.L. contributed equally to this article.

Supplemental material for this article may be found at http://dx.doi.org/10.1128/JVI.01777-14.

doi:10.1128/JVI.01777-14

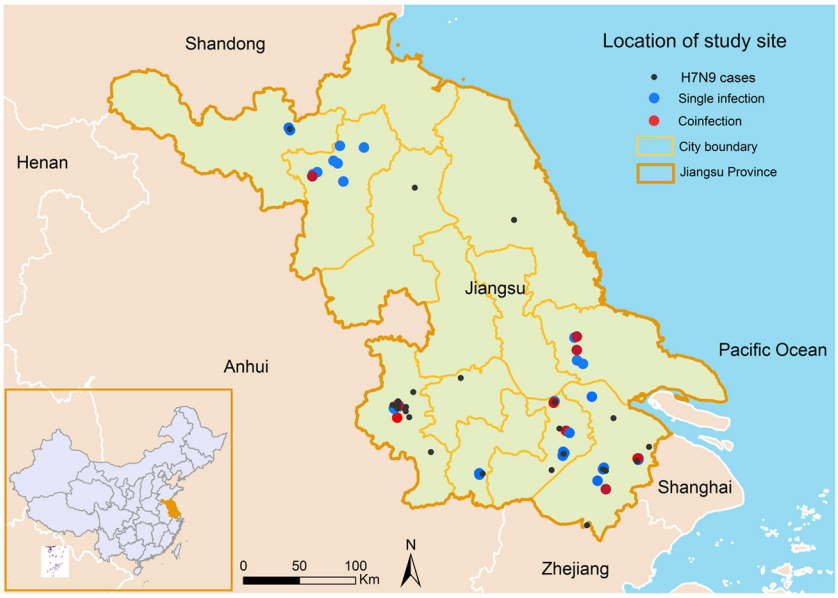

FIG 1 Map of Jiangsu Province, China (Data Sharing Infrastructure of Earth System Science, http://www.geodata.cn/), showing the sites sampled in this study. Blue circles show the locations where birds with H7N9 single infections were found. Red circles show the locations where birds with H7N9/H9N2 coinfection were found. Black circles show the location of human cases of H7N9 infection. The position of Jiangsu province within mainland China is shown in the inset.

quencing. Phylogenetic molecular clock analyses were performed to trace the molecular evolutionary history of the virus and to identify reassortment events.

MATERIALS AND METHODS

Sampling locations. We conducted active surveillance of poultry in Jiangsu province, the epicenter of the H7N9 epidemic where early human cases were reported (Fig. 1). Sampling sites were randomly set at seven live poultry markets and poultry farms where several avian species were available. Four kinds of birds—chicken, duck, goose, and pigeon—were sampled. Cloacal and tracheal swabs and fecal samples were collected. Each sample was placed in 2 ml of minimal essential medium supplemented with penicillin and streptomycin and transferred on ice to the laboratory for detection. A target sample size of 300 was chosen in order to detect a 10% H7N9 prevalence with a 95% confidence interval of ±5%. However, because multiple avian species were surveyed, the target sample size was not reached for each species individually.

Ethics statement. All animal studies were approved by the Institutional Animal Care and Use Committee at Beijing Institute of Microbiology and Epidemiology, Beijing, China, and performed according to institutional guidelines for animal welfare.

Virus detection and subtyping by RT-PCR. Viral RNA extraction was performed from samples using a QIAamp Viral RNA minikit (Qiagen, Maryland, MD, USA), according to the manufacturer's instructions. Briefly, 140 μl of the filtered specimens was mixed with 560 μl of AVL buffer (Qiagen) and incubated for at least 10 min at room temperature. After the addition of 560 μl of absolute ethanol, the mixture was vortexed and applied to a spin column. After washing and drying steps, RNA was eluted in 60 μl of RNase-free water. The RNA samples were subjected to universal detection of type A influenza viruses by quantitative real-time reverse transcription-PCR (RT-qPCR) using WHO-recommended primers and probes (13). To confirm the existence of H9 and N2 in the coinfected samples, two pairs of specific primers for the H9 fragment (H9_2f, 5′-ATCGTCGAGAGACCATCAGC-3′; H9_2r, 5′-GCAGTGTTTGACC CGGTTTT-3′) and N2 fragment (N2_4f, 5′-TGGCGACACACCAAGAG ATG-3′; N2_4r, 5′-GATATTCGCTCCATCAGGCCA-3′) were used to amplify the H9 and N2 genes, and the amplified products were then sequenced by the Sanger method.

Virus isolation and propagation. The swab samples were treated with an antibiotic mixture comprising penicillin (2,000 U/ml), gentamicin (250 μg/ml), and ofloxacin-HCl (60 μg/ml) at 4°C for 24 h. Antibiotic-treated samples (0.2 ml each) were inoculated into the allantoic cavity of 10-day-old specific-pathogen-free (SPF) embryonated chicken eggs for 48 to 72 h at 37°C in order to culture virus. Allantoic fluid of each virus was collected and centrifuged at 3,000 rpm for 5 min at 4°C before storage at −70°C.

Viral genome amplification. Viral genomic RNA extracts from filtered supernatant of virus culture were reverse transcribed into cDNAs, followed by PCR to amplify viral genome sequences using a Superscript One-Step RT-PCR with Platinum *Taq* kit (Invitrogen). A pair of universal full-length primers (MBTuni-12 and MBTuni-13) (14) were used to reverse transcribe and amplify all eight segments of the virus genome. To minimize the risk of contamination, template isolation and PCR setup were performed with specified pipettor sets in separate rooms. Certified RNase-free filter barrier tips were used to prevent aerosol contamination. Nested PCR was avoided, and all PCR assays were performed with appropriate negative controls.

Viral genome sequencing. After one-step RT-PCR amplification, the PCR products were purified with an EZNA Cycle-Pure kit (Omega) and then subjected to next-generation sequencing (NGS) using an Ion Torrent Personal Genome Machine (PGM; Life Technologies, South San Francisco, CA). First, primary cDNA libraries were built with an NEBNext Fast DNA Library Prep Set for Ion Torrent (New England BioLabs, Ipswich, MA) according to the manufacturer's instructions (NEB E6270S/L 10/50 reaction kits). The primary libraries were then diluted to appropriate concentrations for emulsion PCR amplification with an Ion One-Touch 200 Template kit, version 2 DL, on a OneTouch machine (Life Technologies). The emulsion PCR products generated on magnetic beads were then enriched and purified and loaded onto 318 chips (Life Technologies) for parallel sequencing by synthesis using an Ion Torrent PGM (Life Technologies). In total 640 flowgrams were captured, and base calling was performed by PGM built-in software. Raw sequencing data in fastq format were obtained from the PGM and split into individual samples according to the bar code sequences. The genome sequences of the viruses were assembled using Roche 454 Newbler, version 2.8, software (Roche).

Sequence preparation and alignment. All available influenza virus genome nucleotide sequences were downloaded from the GenBank (http://www.ncbi.nlm.nih.gov/GenBank/) and Global Initiative on Sharing Avian Influenza Data (GISAID [http://platform.gisaid.org/]) databases. The sequences were sorted into different gene segments and then combined with the new sequences obtained in this study. Each gene data set was aligned using the MUSCLE program, version 3.5 (15), with manual adjustment.

Initial phylogenetic analysis. An initial large-scale phylogeny was constructed for each large gene data set using RAxML, version 7.8.6. The H7N9 outbreak lineages and our newly sequenced viruses were identified in the global phylogeny, and strains closely related to these were extracted to form a refined alignment that contained all evolutionarily relevant sequences for studying H7N9 emergence. Phylogenies of these smaller data sets were estimated using the maximum-likelihood method and the GTR+I+Γ_4 (general time-reversible model with a proportion of invariant sites and gamma-distributed rate variation across sites) nucleotide substitution model implemented in PhyML, version 3.0 (16). Bootstrap analysis with 1,000 replicates was performed to evaluate the robustness of the estimated phylogenetic topology.

Bayesian molecular clock phylogenetic analysis. To estimate divergence times and rates of nucleotide substitution for influenza A H7N9 viruses, we used the Bayesian Markov chain Monte Carlo method (BMCMC) as implemented in BEAST, version 1.8 (17). A relaxed molecular clock model with uncorrelated log-normally distributed rates (UCLD), the SRD06 (Shapiro-Rambaut-Drummond 2006) nucleotide substitution model, and the Bayesian Skyride demographic model were used (18). We computed out two independent chains for 40 to 80 million generations and sampled 40,000 to 80,000 trees for each chain to ensure adequate effective sample size (>200) of all parameters. MCMC convergence and effective sample sizes were assessed using Tracer, version 1.5 (http://tree.bio.ed.ac.uk). The first 10 to 20% of each chain was discarded as burn-in.

Isolation of H7N9 and H9N2 viruses from coinfected samples. For samples that were shown by RT-PCR to be H7N9/H9N2 coinfected, various approaches were undertaken to characterize both virus strains, including plaque purification and the use of anti-H9N2 antibodies (with the aim of allowing the strain at lower concentration to preferentially propagate). Briefly, confluent monolayer MDCK cells were inoculated at 37°C for 1 h with 10-fold serially diluted samples. Prior to inoculation, the sample was treated with an antibiotic mixture comprising penicillin (2,000 U/ml), gentamicin (250 μg/ml), and ofloxacin-HCl (60 μg/ml) at 4°C for 24 h. After the removal of the inoculum, cells were washed once with phosphate-buffered saline (PBS) and overlaid with 1:1 low-melting-point agarose (1.8%) and 2× Dulbecco's modified Eagle's-F12 (DME-F12) medium supplemented with GlutaMAX (Invitrogen, Carlsbad, CA), insulin-transferrin-selenium (ITS; Invitrogen), and 3 μg/ml acetylated trypsin (Sigma, St. Louis, MO). After the agar was allowed to solidify, the plates were incubated for ~48 h at 37°C and stained with 0.025% neutral red containing 1% agarose. Plaques were then isolated by plaque picking and propagation in SPF chicken embryos. Progeny virus clones (100 per sample) were subjected to reisolation by plaque purification. The H7N9 or H9N2 virus isolates were selected separately after three serial rounds of plaque purification.

For the coinfected samples with significantly higher quantities of H9N2 than H7N9 virus, a chicken polyclonal antibody to H9N2 viruses (Lianshi Biotech Co., Shanghai, China) was applied to neutralize the H9N2 virus for 1 h at 37°C, and then virus was inoculated in MDCK cells for plaque assay and plaque purification. All virus isolation procedures were conducted in a biosafety level 3 facility.

Epidemiological analysis. We used observed-to-expected ratios to determine if the numbers of coinfections were statistically significant (10). The expected number of coinfections under the null hypothesis was calculated as the product of (i) the frequency of H7N9 infections, (ii) the frequency of the H9N2 infections, and (iii) total sample size. The observed-to-expected ratio of the number of coinfections was then used to measure whether specific subtype combinations were more or less likely to coinfect using Fisher's exact test.

Nucleotide sequence accession numbers. The genomic sequences generated in this study have been deposited in the Global Initiative on Sharing Avian Influenza Data (GISAID, http://platform.gisaid.org/) database under accession numbers EPI_ISL_159062 through EPI_ISL_159069.

TABLE 1 Summary of study samples

Host species	No. of samples (tracheal, cloacal, fecal)	No. of samples (tracheal, cloacal, fecal) by subtype (%)[a]		
		H7N9 only	H9N2 only	H7N9/H9N2
Pigeon	28, 32, 62	1, 1, 2 (3.2)	3, 0, 3 (4.9)	1, 0, 0 (0.8)
Chicken	28, 51, 28	0, 4, 0 (3.7)	4, 6, 3 (12)	6, 6, 2 (13)
Duck	13, 18, 9	1, 4, 2 (18)	0, 1, 0 (2.5)	0, 0, 0
Goose	6, 4, 4	1, 0, 0 (7.1)	0, 0, 0	0, 0, 0
Total	283	16 (5.6)	20 (7.1)	15 (4.9)

[a] Based on RT-PCR detection.

RESULTS

A total of 283 tracheal, cloacal, and fecal samples were collected from a variety of birds in poultry markets and farms in Jiangsu province (Table 1), which were subsequently screened for H7N9 and H9N2 subtypes by specific RT-PCR assay. H7N9 viruses were detected in 16 birds (4 chickens, 7 ducks, 1 goose, and 4 pigeons). H9N2 viruses were identified in 20 birds (13 chickens, 1 duck, and 6 pigeons). Significant differences in the frequencies of H7N9 and H9N2 infections among bird species were observed (Fisher's exact test; $P = 0.008$ for H7N9, and $P = 0.013$ for H9N2). Fourteen H7N9/H9N2 coinfections were found. The observed frequency of H7N9/H9N2 coinfection in chickens was significantly higher than that expected under random occurrence, given the observed frequencies of H7N9 and H9N2 viruses we found in chickens (contingency table analysis, Fisher's exact test; $P < 0.001$). Both single infections and coinfections with H7N9 viruses occurred close to locations where human cases have been reported (Fig. 1). By performing H7- and H9-specific amplification with RT-qPCR on coinfected samples, we found that the ratio of H7N9 to H9N2 viruses was between 1:10 and 1:100. Thus, H9N2 appears to be the dominant strain in all coinfected samples.

In order to gain further insights into the molecular evolution of H7N9 viruses, we attempted to isolate and sequence virus from positive samples. Two H7N9 isolates and two H9N2 isolates were obtained from four single-infection samples (samples 759, 761, 503, and 023): A/chicken/Nanjing/759/2013 (H7N9), A/chicken/Nanjing/761/2013 (H7N9), A/chicken/Nanjing/503/2013 (H9N2), and A/chicken/Nantong/023/2013 (H9N2). Isolation was successful for three coinfected samples (samples 097, 106, and 031). For the coinfected samples 031 and 106, a significantly higher quantity of H9N2 virus was present (the ratio of H9N2 to H7N9 was about 100:1, as determined by quantitative RT-PCR). The H7N9 virus could not be isolated from these samples by plaque purification. The samples were then subjected to neutralization using anti-H9N2 antibody, followed by a plaque purification assay. Even with these efforts, only two H9N2 strains (A/chicken/Nanjing/106-2/2013 and A/chicken/Nantong/031-2/2013) were obtained. However, in samples 106 and 031 we did observe H7- and N9-like gene sequences when the original samples were subjected to deep

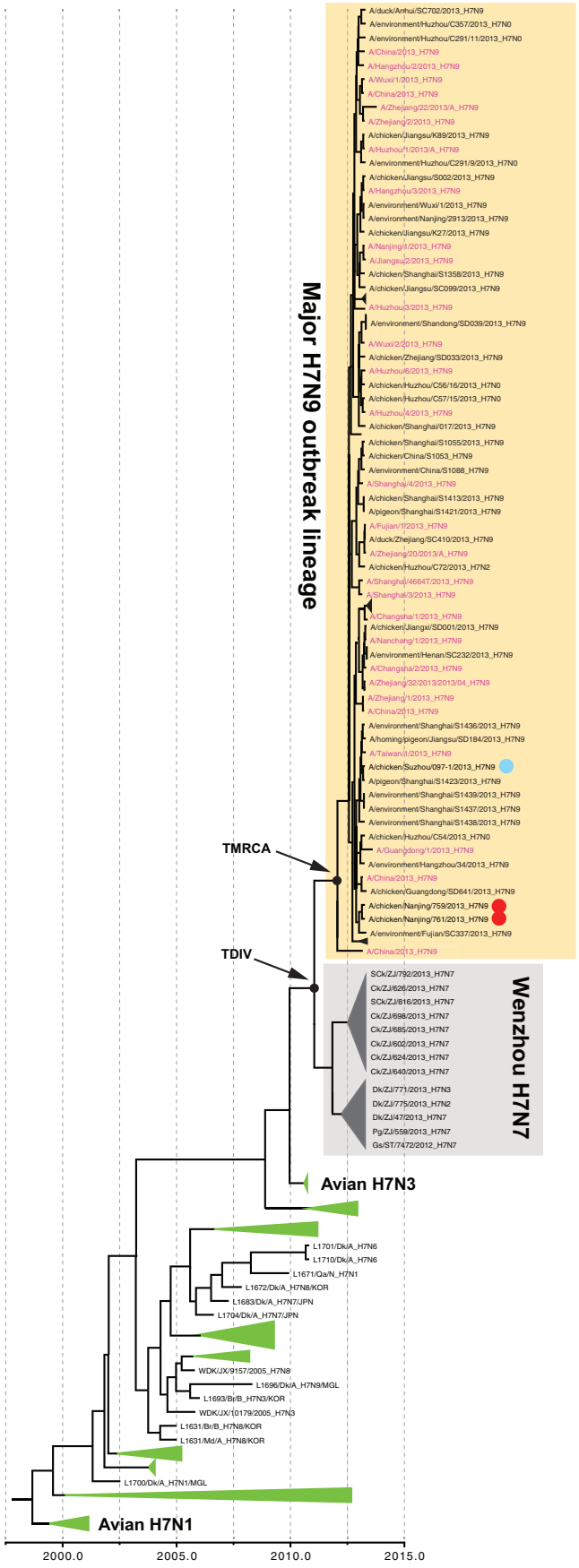

sequencing prior to plaque purification (not studied further here). The complete genomes of these eight virus isolates were sequenced and deposited in the Global Initiative on Sharing Avian Influenza Data (GISAID) database in March 2014 (accession numbers are provided in Table S1 in the supplemental material).

For the remaining coinfected sample (097) with a high titer of H7N9, one H7N9 strain (A/chicken/Suzhou/097-1/2013) and one H9N2 strain (A/chicken/Suzhou/097-2/2013) were obtained by plaque purification. Sample 097 was passaged by experimental inoculation and serial propagation three times in embryonated chicken eggs (100 PFU for each inoculation). Progeny viruses were subjected to plaque purification. A total of 100 clones were obtained from each sample and subjected to genome sequencing. Phylogenetic analyses indicated that the H7N9 strains obtained from the coinfected samples clustered with the major H7N9 outbreak lineage in 7 out of 8 genome segments (Fig. 2 and 3; see also Fig. S1 to S6 in the supplemental material), with the exception of sample 097 (A/chicken/Suzhou/097-1/2013) in the M segment (see Fig. S5). Interestingly, in the M phylogeny, this strain is found in a minor clade that contains a human isolate from Taiwan (A/Taiwan/1/2013/H7N9), as well as other H7N9 avian viruses, with high posterior probability (see Fig. S5), suggesting that an extra reassortment event might have occurred.

In contrast, the H9N2 strains are phylogenetically dispersed and cluster with divergent avian H9N2 lineages (Fig. 3; see also Fig. S1 to S3, S5, S6, and S8 to S10 in the supplemental material). Although the H9N2 strain from the coinfected sample 097 (A/chicken/Suzhou/097-2/2013) typically clusters with other H9N2 avian viruses, in the NP (nucleoprotein) phylogeny it groups with a high posterior probability with H7N9 viruses sampled in 2013 from the environment, together with a human isolate (A/Shanghai/1/2013/H7N9) (Fig. 3). Further, Fig. 3 shows that this cluster is one of several, with posterior support of >0.99, to contain human H7N9 isolates (shown in pink in Fig. 3) outside the major H7N9 outbreak lineage. However, the potential for undersampling precludes a definitive assessment as to when these H7N9 clusters were generated; for example, the cluster containing A/Guangdong/1/2013/H7N9 is preceded by a long branch, indicating substantial unsampled diversity (Fig. 3). Despite this caveat, the cluster comprising poultry infections from Rizhao (China) illustrates that new H7N9 reassortant viruses can be generated by ongoing reassortment between avian H7N9 and H9N2 lineages (Fig. 3).

The time of the most recent common ancestor (TMRCA) of the major H7N9 outbreak lineage was estimated for each segment (Table 2). Table 2 also shows the lineage's time of divergence (TDIV) from all other strains (Fig. 2 highlights the positions of TMRCA and TDIV). The date estimates are broadly consistent among segments but are older for neuraminidase (NA) than for

FIG 2 A molecular clock phylogeny tree of the hemagglutinin (HA) gene of H7N9 viruses sampled from humans and birds during the 2013 outbreak, plus related avian H7 viruses. The tree is a maximum clade credibility tree. Isolate names in pink are H7N9 viruses sampled from humans. Strains sampled in this study are highlighted with circles on the tree: red circles show single infections, and blue circles show mixed infections. Green triangles indicate clusters of influenza viruses sampled from the wild-bird reservoir. Posterior clade probabilities for selected nodes are displayed. Some taxa have been removed from the tree for visual clarity; a full phylogeny with all taxa shown is provided in Fig. S7 in the supplemental material.

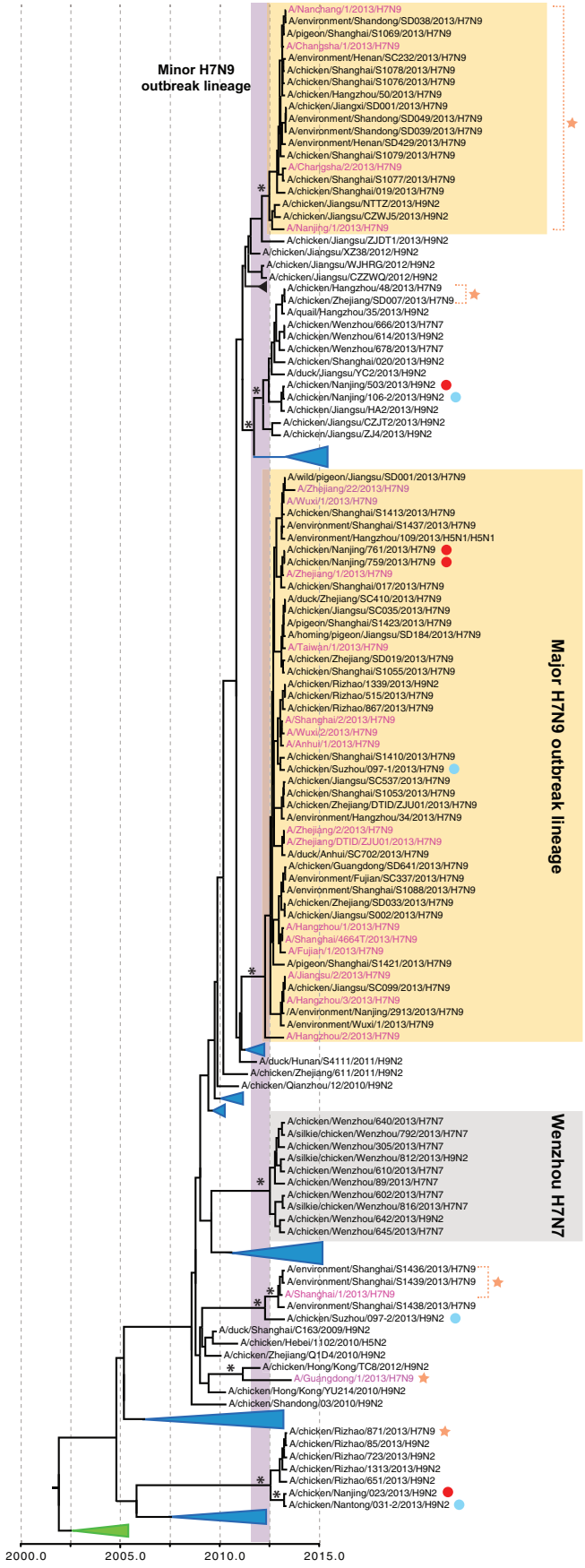

other segments. These results are consistent with previous estimates and indicate that the major outbreak lineage is likely to have emerged between mid-2011 and mid-2012. Figure 4 summarizes the main findings from the time-resolved phylogenies estimated for the H7N9 viruses in this study. Phylogenies for each influenza virus genome segment are shown; in each the major and minor lineages are highlighted in orange and yellow, respectively, and their relative dates of common ancestry are shown (Fig. 4). While the major H7N9 outbreak lineage is observed in all segments, in three of the internal segments (NP, M, and PB1), there is also evidence of a minor outbreak lineage comprising both human and poultry H7N9 infections (Fig. 3; see also Fig. S1 and S5 in the supplemental material). The emergence of the minor H7N9 outbreak lineage is estimated to date between mid-2012 and early 2013 (Fig. 3; see also Fig. S1 and S5) and resulted from reassortment between the major H7N9 outbreak lineage and cocirculating avian H9N2 viruses. This minor lineage was likely generated after the origin of the major outbreak lineage because the MRCA of the major lineage is older (between mid-2011 and mid 2012) (Table 2 and Fig. 4). Future surveillance of the current H7N9 epidemic may likely reveal other H7N9 lineages that are continually being generated by reassortment.

Genome analysis revealed that the hemagglutinin (HA) genes of all the H7N9 viruses obtained in this study have acquired the "human-like" residue leucine at position 226 but have retained the "avian-like" residue glycine at position 228 at the HA receptor site (H3 numbering) (see Fig. S5 in the supplemental material), implying that these viruses have partially acquired binding specificity for human receptors (2). The lack of an HA multibasic cleavage site, which is a molecular signature conferring high pathogenicity, suggests that these viruses have low pathogenicity in avian populations (6). All of the H7N9 viruses sequenced in this study have a 627E residue in the PB2 protein, instead of the mammalian-adapted 627K mutation that is present in many (47/70) human isolates (see Fig. S6). Like most published H7N9 strains, all of the strains sequenced here lacked the R292K mutation in NA and carried the S31N residue in the M2 gene, which means that they are probably sensitive to oseltamivir and resistant to amantadine (13, 19).

DISCUSSION

Coinfection of influenza A viruses in wild and domestic birds is thought to be an important condition for the diversification of influenza virus phenotypes by reassortment (10, 20). Such a mechanism was responsible for development of the highly pathogenic H5N1 avian influenza virus that appeared in Hong Kong in 1997, which was derived from the reassortment of the H5 gene

FIG 3 A molecular clock phylogeny tree of the nucleoprotein (NP) gene of avian influenza viruses related to the human and avian H7N9 viruses sampled during the 2013 outbreak. The tree is a maximum clade credibility tree. Isolate names in pink are H7N9 viruses sampled from humans. Strains sampled in this study are highlighted with circles on the tree: red circles show single infections, and blue circles show mixed infections. Furthermore, the minor H7N9 lineages are highlighted by orange stars, and time of emergence of the major outbreak lineage is indicated by the purple vertical bar. Blue triangles indicate clusters of avian H9N2 viruses while green triangles indicate clusters of influenza viruses sampled from the wild-bird reservoir. Posterior clade probabilities for selected nodes are displayed. Some taxon names are not displayed for visual clarity. A full phylogeny with all taxon names shown is provided in Fig. S8 in the supplemental material.

TABLE 2 Divergence time estimates for each segment of the 2013 major H7N9 human outbreak

Gene	TDIV (mo yr [95% HPD])[a]	TMRCA (mo yr [95% HPD])[a]	Mean evolutionary rate (10^{-3} substitutions/site/yr [95% HPD])
PB2	Nov. 2011 (July 2011, Mar. 2012)	Mar. 2012 (Nov. 2011, July 2012)	3.32 (2.88, 3.77)
PB1	July 2011 (Nov. 2010, Feb. 2012)	Mar. 2012 (Sept. 2011, July 2012)	3.97 (3.49, 4.45)
PA	Dec. 2011 (July 2011, May 2012)	June 2012 (Feb. 2012, Sept. 2012)	3.77 (3.27, 4.30)
HA	Jan. 2011 (May 2010, Aug. 2011)	Jan. 2012 (July 2011, May 2012)	5.22 (4.71, 5.72)
NP	Feb. 2011 (Sept. 2010, May 2011)[c]	Apr. 2012 (Sept. 2011, Aug. 2012)	3.35 (2.92, 3.80)
NA	Oct. 2010 (Nov. 2009, July 2011)	Oct. 2011 (Dec. 2010, Feb. 2012)	3.07 (2.36, 3.83)
MP	Sept. 2011 (Mar. 2011, Mar. 2012)	Feb. 2012 (Oct. 2011, July 2012)	3.48 (2.86, 4.11)
NS	May 2011 (Sept. 2010, Jan. 2011)[b]	Feb. 2012 (Sept. 2011, June 2012)	3.57 (3.05, 4.12)

[a] Estimated dates are shown for the time of divergence (TDIV) and time of most recent common ancestor (TMRCA) of the H7N9 outbreak lineage. All data are node supported by a posterior probability of >0.95 except as noted. HPD, highest posterior density.
[b] Node supported by a posterior probability of >0.85.
[c] Node supported by a posterior probability of <0.5.

from H5N1 viruses, the N1 gene from H6N1 viruses, and internal genes from H9N2 viruses (21, 22). This study is the first report of the molecular epidemiology of cocirculating H7N9 and H9N2 viruses in poultry populations at Jiangsu, an epicenter of the H7N9 epidemic where early human infections were reported. We found that H7N9/H9N2 coinfection occurred frequently, yet almost all instances of coinfection were in chickens, indicating that chickens, rather than other birds, represent the most probable

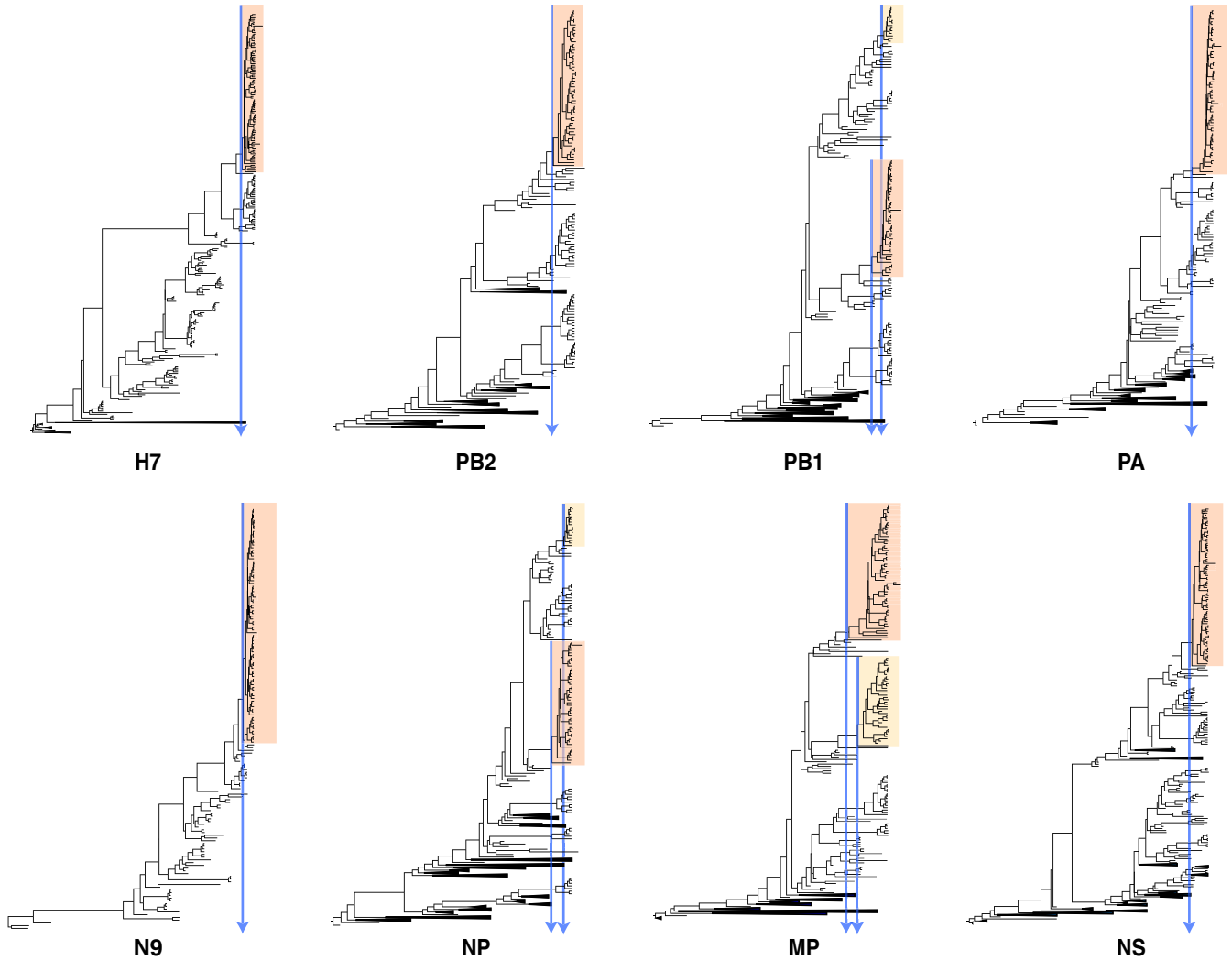

FIG 4 A schematic summarizing the main findings inferred from the time-resolved phylogenies of the H7N9 viruses sampled from poultry and humans (full phylogenies are provided in Fig. S1 to S10 in the supplemental material). The major and minor outbreak lineages are highlighted in orange and yellow, respectively. The blue arrows indicate the times of the most recent common ancestors of these lineages, illustrating that the minor lineage is likely to have arisen after the emergence of the major lineage, which supports the hypothesis of ongoing reassortment among H7N9 and cocirculating viral lineages. MP, matrix protein.

mixing vessel of the two viral subtypes. It is surprising that the observed frequency of H7N9/H9N2 coinfection in chickens was significantly higher than expected as it has been previously shown that a well-adapted influenza virus in an infected bird can restrict coinfection by another strain, and thus observed coinfections might be expected, *a priori*, to be rare (5). On the other hand, H9N2 appears to be the dominant strain in all coinfected samples, suggesting the hypothesis that H9N2 is better adapted than H7N9 during coinfection of both subtypes in chickens though the H7N9 strain is not being competitively excluded.

The phylogenetic analysis results suggest that there have been several opportunities for different H7N9 reassortant viruses to initiate widespread transmission in birds and humans, but only one lineage (the major outbreak lineage) has been highly successful. For example, inspection of the NP phylogeny identifies at least five distinct H7N9 lineages that were generated around the time that the major outbreak lineage emerged in poultry and humans (highlighted by orange stars in Fig. 3).

The strains isolated from the coinfected sample 097 highlight the complex origins of the outbreak lineage, whose identity is made complex by ongoing reassortment with the contemporaneous avian viral reservoir. The number of coinfections sampled in chickens in this study suggests that coinfection with antigenically distinct strains may be common in the domestic avian reservoir.

For the coinfected sample 097, it is intriguing that although the H9N2 virus was dominant in the original sample, as demonstrated by RT-PCR, only H7N9 virus was isolated after inoculation of the sample in chicken embryos (see Materials and Methods). Further, two different reassortant H7N9 genotypes were isolated after serial propagation in embryonated chicken eggs of the original sample, as revealed by RT-PCR analysis of individual progeny virus clones. The dominant genotype (90% of total isolates, as revealed by RT-qPCR) harbored PB2 and PB1 segments from the original H9N2 virus, while the minority genotype acquired only PB1 from the original H9N2 virus. The original, nonreassortant H7N9 virus was no longer observed in the serially propagated culture. This suggests that during growth in culture, the PB1 and PB2 segments of the locally circulating H9N2 virus reassorted with the original H7N9 virus, and the resulting reassortant replaced the original H7N9 and H9N2 strains, perhaps because it can grow more rapidly in chicken embryos at 37°C. However, we are not able to determine whether the reassortment event occurred within the sampled avian host or *in vitro* during passage in chicken embryos. The reassortant genomes observed were not monotypic after only three passages, suggesting that the reassortment process was complex and dynamic.

Taken together, the occurrence of H7N9/H9N2 coinfection observed in our survey suggests that the reassortment process is ongoing. The high prevalence, broad host range, and high genetic diversity of H9N2 avian influenza viruses in the epidemic center mean that they continue to represent a source of further genetic diversity for H7N9 viruses through reassortment and thus may be involved in future epidemic and pandemic strains. We stress the need for surveillance of all avian influenza virus subtypes, especially in chickens, using whole-genome sequences in order to detect novel reassortment combinations. The results presented here concerning H7N9/H9N2 competition during coinfection are circumstantial and remain to be formally validated by viral challenge experiments using immunologically naive birds under controlled conditions. Whether the newly generated H7N9 virus and its reassortants possess bird species-specific transmissibility or pathogenicity also requires future investigation.

This study reflects the unavoidable constraints placed on field sampling in the period immediately following the discovery of the novel H7N9 virus in humans. Convenience sampling was undertaken at live poultry markets and poultry farms, from which the number of accessible samples was limited. The small sampling size prevents us from deriving formal population-level estimates of the prevalence of H7N9/H9N2 coinfection. In particular, the sample sizes from geese are low and may not reflect the true ecological circumstances in the sampled region.

ACKNOWLEDGMENTS

We are grateful to the Chinese National Influenza Center, Chinese CDC, for sharing the 2013 China H7N9 influenza virus strain sequences deposited in the GISAID database. We thank all of the personnel who contributed to sample collection.

We acknowledge the support of the National Ministry of Science and Technology Emergency Research Project on human infection with avian influenza H7N9 virus (grant KJYJ-2013-01-02) and the China Mega-Project on Infectious Disease Prevention (grants 2013ZX10004-202 and 2013ZX10004-605).

We declare that we do not have any commercial or other association that might pose a conflict of interest.

All authors read and approved the final manuscript.

REFERENCES

1. **Tu C, Fu L, Tang R, He T, Chen J, Fang Y, Wang J, Huang Z.** 2014. The first case of avian influenza A (H7N9) virus occurring in the autumn season, China. Am. J. Infect. Control **42:**212–213. http://dx.doi.org/10.1016/j.ajic.2013.10.002.
2. **Chen Y, Liang W, Yang S, Wu N, Gao H, Sheng J, Yao H, Wo J, Fang Q, Cui D, Li Y, Yao X, Zhang Y, Wu H, Zheng S, Diao H, Xia S, Zhang Y, Chan KH, Tsoi HW, Teng JL, Song W, Wang P, Lau SY, Zheng M, Chan JF, To KK, Chen H, Li L, Yuen KY.** 2013. Human infections with the emerging avian influenza A H7N9 virus from wet market poultry: clinical analysis and characterisation of viral genome. Lancet **381:**1916–1925. http://dx.doi.org/10.1016/S0140-6736(13)60903-4.
3. **Gao R, Cao B, Hu Y, Feng Z, Wang D, Hu W, Chen J, Jie Z, Qiu H, Xu K, Xu X, Lu H, Zhu W, Gao Z, Xiang N, Shen Y, He Z, Gu Y, Zhang Z, Yang Y, Zhao X, Zhou L, Li X, Zou S, Zhang Y, Li X, Yang L, Guo J, Dong J, Li Q, Dong L, Zhu Y, Bai T, Wang S, Hao P, Yang W, Zhang Y, Han J, Yu H, Li D, Gao GF, Wu G, Wang Y, Yuan Z, Shu Y.** 2013. Human infection with a novel avian-origin influenza A (H7N9) virus. N. Engl. J. Med. **368:**1888–1897. http://dx.doi.org/10.1056/NEJMoa1304459.
4. **Li Q, Zhou L, Zhou M, Chen Z, Li F, Wu H, Xiang N, Chen E, Tang F, Wang D, Meng L, Hong Z, Tu W, Cao Y, Li L, Ding F, Liu B, Wang M, Xie R, Gao R, Li X, Bai T, Zou S, He J, Hu J, Xu Y, Chai C, Wang S, Gao Y, Jin L, Zhang Y, Luo H, Yu H, He J, Li Q, Wang X, Gao L, Pang X, Liu G, Yan Y, Yuan H, Shu Y, Yang W, Wang Y, Wu F, Uyeki TM, Feng Z.** 2014. Epidemiology of human infections with avian influenza A(H7N9) virus in China. N. Engl. J. Med. **370:**520–532. http://dx.doi.org/10.1056/NEJMoa1304617.
5. **Liu D, Shi W, Shi Y, Wang D, Xiao H, Li W, Bi Y, Wu Y, Li X, Yan J, Liu W, Zhao G, Yang W, Wang Y, Ma J, Shu Y, Lei F, Gao GF.** 2013. Origin and diversity of novel avian influenza A H7N9 viruses causing human infection: phylogenetic, structural, and coalescent analyses. Lancet **381:**1926–1932. http://dx.doi.org/10.1016/S0140-6736(13)60938-1.
6. **Shi J, Deng G, Liu P, Zhou J, Guan L, Li W, Li X, Guo J, Wang G, Fan J, Wang J, Li Y, Jiang Y, Liu L, Tian G, Li C, Chen H.** 2013. Isolation and characterization of H7N9 viruses from live poultry markets—implication of the source of current H7N9 infection in humans. Chin. Sci. Bull. **58:**1857–1863. http://dx.doi.org/10.1007/s11434-013-5873-4.
7. **Lam TT, Wang J, Shen Y, Zhou B, Duan L, Cheung CL, Ma C, Lycett SJ, Leung CY, Chen X, Li L, Hong W, Chai Y, Zhou L, Liang H, Ou Z, Liu Y, Farooqui A, Kelvin DJ, Poon LL, Smith DK, Pybus OG, Leung GM, Shu Y, Webster RG, Webby RJ, Peiris JS, Rambaut A, Zhu H, Guan Y.** 2013. The genesis and source of the H7N9 influenza viruses

causing human infections in China. Nature **502:**241–244. http://dx.doi.org/10.1038/nature12515.

8. **Cui L, Liu D, Shi W, Pan J, Qi X, Li X, Guo X, Zhou M, Li W, Li J, Haywood J, Xiao H, Yu X, Pu X, Wu Y, Yu H, Zhao K, Zhu Y, Wu B, Jin T, Shi Z, Tang F, Zhu F, Sun Q, Wu L, Yang R, Yan J, Lei F, Zhu B, Liu W, Ma J, Wang H, Gao GF.** 2014. Dynamic reassortments and genetic heterogeneity of the human-infecting influenza A (H7N9) virus. Nat. Commun. **5:**3142. http://dx.doi.org/10.1038/ncomms4142.
9. **Zhang L, Zhang Z, Weng Z.** 2013. Rapid reassortment of internal genes in avian influenza A(H7N9) virus. Clin. Infect. Dis. **57:**1059–1061. http://dx.doi.org/10.1093/cid/cit414.
10. **Sharp GB, Kawaoka Y, Jones DJ, Bean WJ, Pryor SP, Hinshaw V, Webster RG.** 1997. Coinfection of wild ducks by influenza A viruses: distribution patterns and biological significance. J. Virol. **71:**6128–6135.
11. **Yu X, Jin T, Cui Y, Pu X, Li J, Xu J, Liu G, Jia H, Liu D, Song S, Yu Y, Xie L, Huang R, Ding H, Kou Y, Zhou Y, Wang Y, Xu X, Yin Y, Wang J, Guo C, Yang X, Hu L, Wu X, Wang H, Liu J, Zhao G, Zhou J, Pan J, Gao GF, Yang R, Wang J.** 2014. Influenza H7N9 and H9N2 viruses: coexistence in poultry linked to human H7N9 infection and genome characteristics. J. Virol. **88:**3423–3431. http://dx.doi.org/10.1128/JVI.02059-13.
12. **Lu J, Wu J, Zeng X, Guan D, Zou L, Yi L, Liang L, Ni H, Kang M, Zhang X, Zhong H, He X, Monagin C, Lin J, Ke C.** 2014. Continuing reassortment leads to the genetic diversity of influenza virus H7N9 in Guangdong, China. J. Virol. **88:**8297–8306. http://dx.doi.org/10.1128/JVI.00630-14.
13. **WHO.** 2013. Real-time RT-PCR protocol for the detection of avian influenza A(H7N9) virus. WHO Collaborating Center for Reference and Research on Influenza, Beijing, China. http://www.who.int/influenza/gisrs_laboratory/cnic_realtime_rt_pcr_protocol_a_h7n9.pdf.
14. **Zhou B, Donnelly ME, Scholes DT, St George K, Hatta M, Kawaoka Y, Wentworth DE.** 2009. Single-reaction genomic amplification accelerates sequencing and vaccine production for classical and Swine origin human influenza a viruses. J. Virol. **83:**10309–10313. http://dx.doi.org/10.1128/JVI.01109-09.
15. **Edgar RC.** 2004. MUSCLE: multiple sequence alignment with high accuracy and high throughput. Nucleic Acids Res. **32:**1792–1797. http://dx.doi.org/10.1093/nar/gkh340.
16. **Guindon S, Dufayard JF, Lefort V, Anisimova M, Hordijk W, Gascuel O.** 2010. New algorithms and methods to estimate maximum-likelihood phylogenies: assessing the performance of PhyML 3.0. Syst. Biol. **59:**307–321. http://dx.doi.org/10.1093/sysbio/syq010.
17. **Drummond AJ, Rambaut A.** 2007. BEAST: Bayesian evolutionary analysis by sampling trees. BMC Evol. Biol. **7:**214. http://dx.doi.org/10.1186/1471-2148-7-214.
18. **Shapiro B, Rambaut A, Drummond AJ.** 2006. Choosing appropriate substitution models for the phylogenetic analysis of protein-coding sequences. Mol. Biol. Evol. **23:**7–9. http://dx.doi.org/10.1093/molbev/msj021.
19. **Zhang Q, Shi J, Deng G, Guo J, Zeng X, He X, Kong H, Gu C, Li X, Liu J, Wang G, Chen Y, Liu L, Liang L, Li Y, Fan J, Wang J, Li W, Guan L, Li Q, Yang H, Chen P, Jiang L, Guan Y, Xin X, Jiang Y, Tian G, Wang X, Qiao C, Li C, Bu Z, Chen H.** 2013. H7N9 influenza viruses are transmissible in ferrets by respiratory droplet. Science **341:**410–414. http://dx.doi.org/10.1126/science.1240532.
20. **Kayali G, Kandeil A, El-Shesheny R, Kayed AS, Gomaa MM, Maatouq AM, Shehata MM, Moatasim Y, Bagato O, Cai Z, Rubrum A, Kutkat MA, McKenzie PP, Webster RG, Webby RJ, Ali MA.** 2014. Active surveillance for avian influenza virus, Egypt, 2010–2012. Emerg. Infect. Dis. **20:**542–551. http://dx.doi.org/10.3201/eid2004.131295.
21. **Belser JA, Blixt O, Chen LM, Pappas C, Maines TR, Van Hoeven N, Donis R, Busch J, McBride R, Paulson JC, Katz JM, Tumpey TM.** 2008. Contemporary North American influenza H7 viruses possess human receptor specificity: Implications for virus transmissibility. Proc. Natl. Acad. Sci. U. S. A. **105:**7558–7563. http://dx.doi.org/10.1073/pnas.0801259105.
22. **Zhang P, Tang Y, Liu X, Liu W, Zhang X, Liu H, Peng D, Gao S, Wu Y, Zhang L, Lu S, Liu X.** 2009. A novel genotype H9N2 influenza virus possessing human H5N1 internal genomes has been circulating in poultry in eastern China since 1998. J. Virol. **83:**8428–8438. http://dx.doi.org/10.1128/JVI.00659-09.